J. Wang, P. Munankarmi, J. Maguire, C. Shi, W. Zuo, D. Roberts, X. Jin 2022."Carbon Emission Responsive Building Control : A Case Study With an All-Electric Residential Community in a Cold Climate," Applied Energy, 314, pp. 118910, https://doi.org/10.1016/j.apenergy.2022.118910

Carbon Emission Responsive Building Control: A Case Study With an All-Electric Residential Community in a Cold Climate

Jing Wang[a,b], Prateek Munankarmi[b], Jeff Maguire[b], Chengnan Shi[a], Wangda Zuo[a,b], David Roberts[b], Xin Jin[b,*]

[a]*Department of Civil, Environmental and Architectural Engineering, University of Colorado Boulder, 1111 Engineering Dr, Boulder, 80309, CO, United States*
[b]*National Renewable Energy Laboratory, 15013 Denver West Parkway, Golden, 80401, CO, United States*

Abstract

In the United States, buildings account for 35% of total energy-related carbon dioxide emissions, making them important contributors to decarbonization. Carbon intensities in the power grid are time-varying and can fluctuate significantly within hours, so shifting building loads in response to the carbon intensities can reduce a building's operational carbon emissions. This paper presents a rule-based carbon responsive control framework that controls the setpoints of thermostatically controlled loads responding to the grid's carbon emission signals in real time. Based on this framework, four controllers are proposed with different combinations of carbon accounting methods and control rules. To evaluate their performance, we performed simulation studies using models of a 27-home, all-electric, net zero energy residential community located in Basalt, Colorado, United States. The carbon intensity data of four future years from the Cambium data set are adopted to account for the evolving resource mix in the power grid. Various performance metrics, including energy consumption, carbon emission, energy cost, and thermal discomfort, were used to evaluate the performance of the controllers. Sensitivity analysis was also conducted to determine how the control thresholds and intervals affect the controllers' performance. Simulation results indicate that the carbon responsive controllers can reduce the homes' annual carbon emissions by 6.0% to 20.5%. However, the energy consumption increased by 0.9% to 6.7%, except in one scenario where it decreased by 2.2%. Compared to the baseline, the change in energy cost was between -2.9% and 3.4%, and thermal discomfort was also maintained within an acceptable range. The little impact on energy cost and thermal discomfort indicates there are no potential roadblocks for customer acceptance when rolling out the controllers in utility programs.

Keywords: Decarbonization, Building control, Rule-based control, Residential community, Carbon accounting

1. Introduction

Buildings account for 35% of carbon dioxide (CO_2) emissions in the United States, which makes buildings important contributors to decarbonization [1]. With the Biden administration's aggressive goal to reduce 50%–52% of greenhouse gas pollution by 2030 [2], a joint effort between the buildings and the electricity sector is emerging to tackle this challenge. Further, the U.S. Department of Energy has developed a roadmap with recommendations for how *Grid-interactive Efficient Buildings* (GEBs) can provide a clean and flexible energy resource [3]. On one side, the power generation is adopting more renewable energy, which is cleaner than traditional coal and natural gas fired plants. On the other side, buildings can reduce their carbon emissions through using less energy (e.g., adoption of energy efficiency measures) or using cleaner energy (e.g., load shifting to cleaner hours).

Building decarbonization can be achieved during various phases of the building life cycle, including design, retrofit, and operation. The design phase often incorporates carbon analysis into early design building energy models [4], and some of the studies focus on embodied carbon emission reduction [5]. For the retrofit phase, several studies have been reported to optimally adopt energy efficiency measures, building system electrification, and high renewable penetration in existing communities for the purpose of enhancing energy performance while attaining carbon neutrality [6, 7, 8, 9, 10].

The above two phases are generally static and concern the long-term carbon emission performance of the buildings. During the building operation phase, carbon responsive building control is more flexible and its deployment requires less capital investment. Adopting carbon emission reductions as one of the objectives or control inputs in optimization-based building control has received increased attention in the last decade [11, 12, 13, 14, 15]. Jin et al. [16] proposed a user-centric home energy management system that is based on a multi-objective model predictive control (MPC) framework. Carbon emission reduction serves as one of the objectives along with the minimization of energy cost, thermal discomfort, and user inconvenience. Leerbeck et al. [17] developed an optimal heat pump controller for building space heating. Using weather and CO_2 emission forecasts as inputs to an MPC, approximately 16% of CO_2 emissions were saved compared to typical thermostatic control.

Despite the rapid development of optimization-based control methods, rule-based control is still the dominant control method in building automation systems due to ease of implementa-

*Corresponding author.
Email address: xin.jin@nrel.gov (Xin Jin)

tion. For example, Clauß [18] investigated predictive rule-based control for reducing the annual CO_2 equivalent greenhouse gas emissions ($CO_{2eq.}$) for a Norwegian single-family detached house. The controlled object was the building heat pump system. Historical weather and $CO_{2eq.}$ emission data from 2015 were used for simulations. The results showed that the carbon responsive control cannot reduce the yearly $CO_{2eq.}$ emission due to the limited daily fluctuations in the average $CO_{2eq.}$ intensity of the Norwegian electricity generation mix.

Carbon accounting methods play an important role in carbon responsive building control. Although electricity net-metering has been broadly taken into account in utility bill calculations, carbon accounting methods have seldom been discussed in the literature. The emissions reduction effect of clean electricity backfeeding to the grid has generally been neglected in the design and evaluation of carbon responsive controllers. Additionally, historical CO_2 emission data are typically adopted in existing studies [18]. With the increasing penetration of renewable energy in the power grid, it is worth exploring evolving emission forecasts and their impact on control strategies. The table below compares this study with existing relevant carbon emission driven control studies.

Table 1: Comparison of existing carbon emission driven control studies.

Ref.	Predictive control	CO_2 forecast	Carbon net-metering
[11]	✗	✗	✗
[12, 16, 18]	✓	✗	✗
[13, 14, 15, 17]	✓	✓	✗
This paper	✓	✓	✓

In this paper, we propose a rule-based carbon responsive control framework to reduce the carbon emissions of residential buildings. Real-time carbon emission data are utilized to inform the setpoint control of thermostatically controlled loads such as heating, ventilation, and air-conditioning (HVAC) systems and water heating (WH) systems. More specifically, the impact of carbon accounting methods such as carbon net-metering is studied through the design of various control algorithms. Both momentary and predictive rule-based controllers are evaluated to study the value of prediction in real-time carbon responsive control. In the case study, models for an all-electric residential community of 27 homes located in Basalt, Colorado, are adopted for control implementation and evaluation. Additionally, the evolving resource mix in the power grid is considered in the simulation scenarios. The major contributions of this paper include:

- Development of a carbon emission responsive control framework for decarbonizing residential buildings;
- Demonstration of the control framework in a simulated all-electric residential community in a cold climate;
- Evaluation of the impact of carbon accounting methods and control rules on emission, energy, cost, and discomfort;
- Forecasting of the community's future carbon emissions with the evolving resource mix in the power grid.

The remainder of this paper is organized as follows: Section 2 presents the research methodology of the proposed rule-based carbon responsive control framework. The co-simulation platform is also described in that section. Section 3 describes the community energy model and the simulation inputs for the case study. Section 4 discusses the simulation results with various metrics such as energy, carbon, cost, and discomfort along with a sensitivity analysis. Section 5 concludes the work and recommends future topics for further study.

2. Methodology

2.1. Overview of the research methodology

Rule-based carbon emission responsive control, by definition, is to make control decisions in response to real-time carbon emission signals following certain predetermined rules. The control objective is to reduce the carbon emission induced by the power usage of the controlled objects, which are thermostatically controlled loads in this work. The thermostat setpoint is controlled to increase or decrease the load depending on the carbon intensities, predetermined rules, and operation modes.

During the design of the carbon responsive control rule, a fundamental step is to determine how the setpoints change with the emission signal. A common method is to divide the carbon emission data range into several regions, where each region correlates with one setpoint [18]. Evolved from this logic, the ultimate rule form is to establish a function (most likely linear) that maps emissions to a set of setpoints. In this paper, we adopt a three-region design of the control rule, which means dividing the carbon emission data range into three regions with two thresholds. Between the lower threshold (LT) and the higher threshold (HT) is the default zone where the default setpoints $T_{set,default}$ (Table 2) will be implemented. Below the LT will be the clean zone and the $T_{set,clean}$ will be implemented, and vice versa. We designed the $T_{set,clean}$ and $T_{set,unclean}$ to be 0.8°C (1.5°F) around $T_{set,default}$ for space heating and cooling, and 8.3°C (15°F) for the water heater. Here we note that the default setpoints should be dependent on the region and user preferences.

Table 2: Control setpoints for heating, cooling, and water heating.

Controlled object	$T_{set,default}$ (°C)	$T_{set,clean}$ (°C)	$T_{set,unclean}$ (°C)
Space heating	21.1	21.9	20.3
Space cooling	23.9	23.1	24.7
Water heater	51.7	60.0	43.4

2.1.1. Carbon accounting methods

Unlike energy net-metering, which has been extensively studied in building-to-grid related control studies, the inclusion of carbon net-metering is relatively rare. To address this research gap, we consider different controller design with and without carbon net-metering to investigate its impact on the control performance.

For electricity prosumers who both consume and produce electricity, carbon net-metering means metering the net carbon

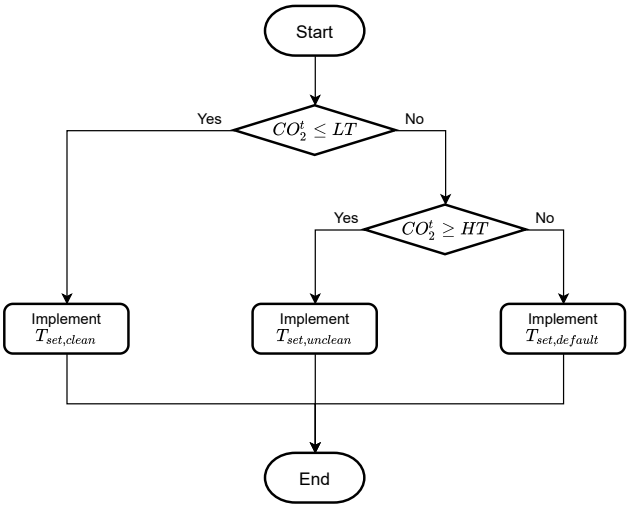

Figure 1: Flow chart of momentary control with carbon net-metering.

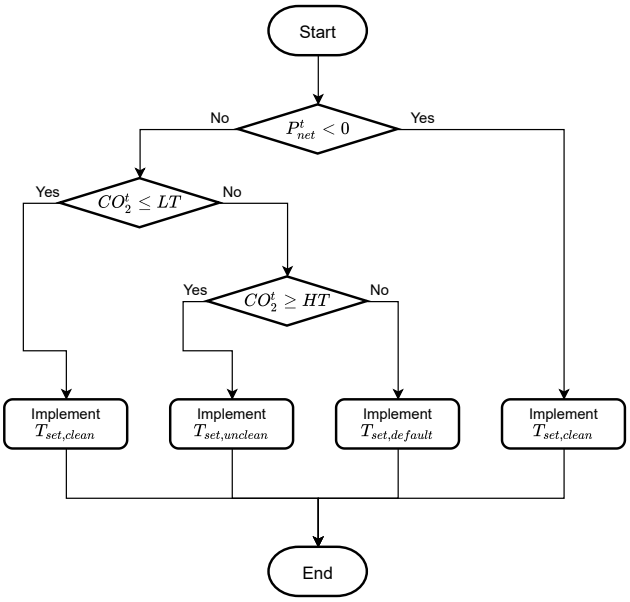

Figure 2: Flow chart of momentary control without carbon net-metering.

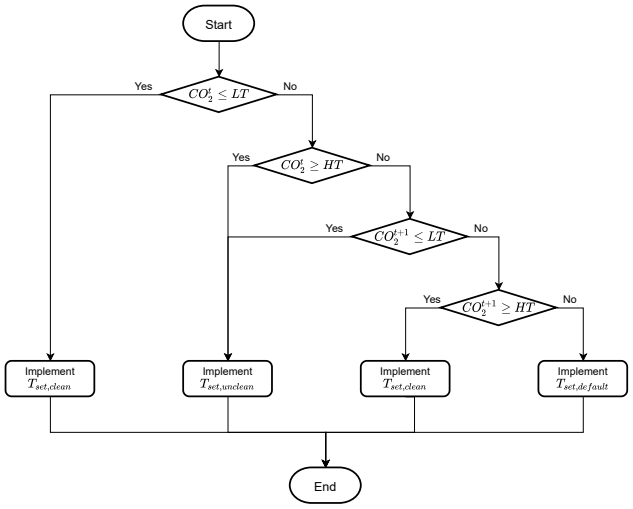

Figure 3: Flow chart of predictive control with carbon net-metering.

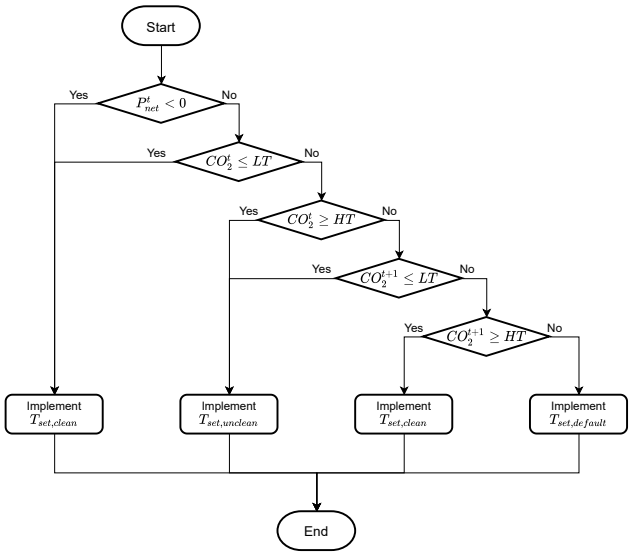

Figure 4: Flow chart of predictive control without carbon net-metering.

emission caused by their electricity consumption and production [19]. In other words, exporting electricity back to the grid will offset carbon emissions from their total emissions. On the contrary, when carbon net-metering is not included, it is more advantageous to use the locally generated electricity from photovoltaic (PV) systems instead of exporting due to the lack of emission benefits. For controllers considering carbon net-metering, it makes no difference whether to use the clean PV energy locally or to export it to the grid. Both options would bring in the same amount of carbon emission reduction.

2.1.2. Control rules

According to the information used for making control decisions, rule-based control can be categorized into momentary and predictive control. The momentary rule-based control adopts the current value of the boundary condition (e.g., carbon emission signal) and decides the setpoints for the current control interval [20]. Nevertheless, the predictive rule-based control makes decisions based on both current and future predictions of the boundary condition [18]. Compared to optimization-based controllers such as MPC, predictive rule-based control is simpler but still effective. It is therefore a promising alternative to MPC given that the rules are well designed [21].

In this work, we propose both momentary and predictive carbon responsive controllers. For the predictive controller, the carbon emission information of one future timestep is adopted to facilitate the determination of setpoints for the current timestep. The detailed control algorithms of the four proposed controllers are discussed in the following subsection.

2.2. Implementation of control algorithms

Figures 1–4 present the flow charts of the four proposed carbon responsive controllers. Here, the LT and HT are predeter-

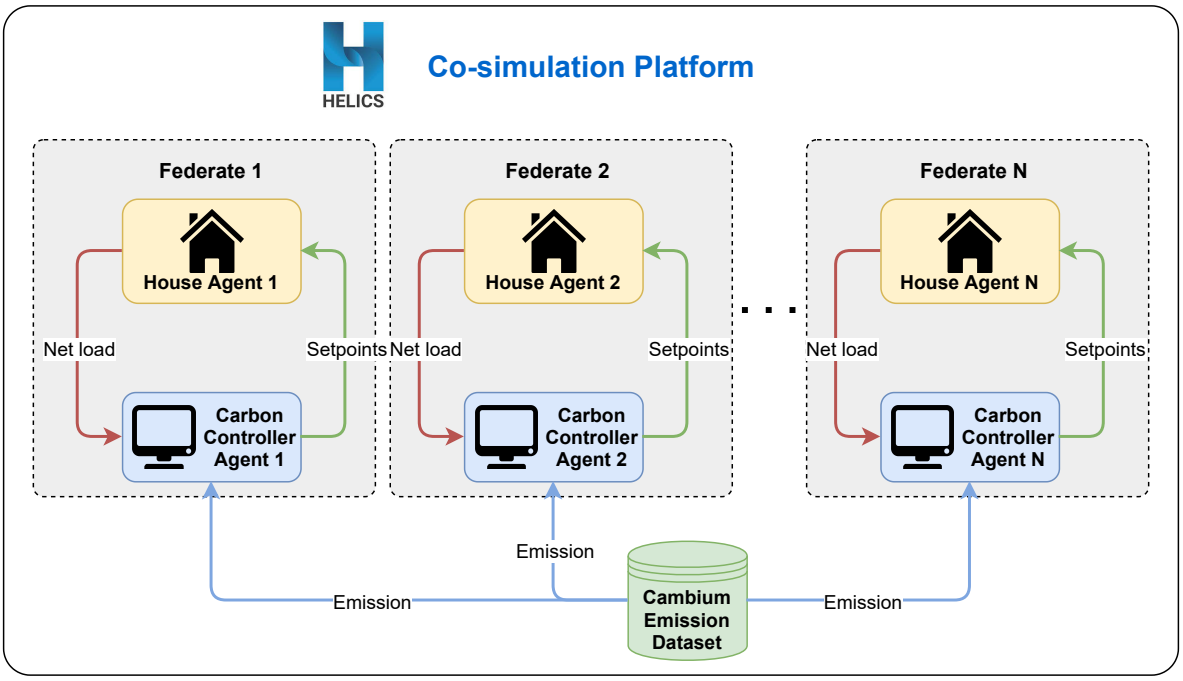

Figure 5: Architecture of the co-simulation platform.

mined thresholds that are held constant throughout the whole simulation period. In the momentary controller with carbon net-metering (Figure 1), the current carbon emission value CO_2^t is compared with the LT and HT sequentially to determine which range it belongs to. If CO_2^t is below the LT, the current timestep will be categorized as clean and the setpoints $T_{set,clean}$ in Table 2 will thus be implemented. As a result, the loads P_{hvac}^t and P_{wh}^t will be increased and vice versa. If CO_2^t is between the LT and HT, the default setpoints $T_{set,default}$ will be implemented, which is the same as the baseline setpoints.

The momentary controller without net-metering (Figure 2) is developed based on the one with net-metering with one more step to increase the PV self-consumption rate. Prior to comparing CO_2^t with the thresholds, the current house net load P_{net}^t is first evaluated. If it is negative, which means the house has surplus PV generation, the setpoints $T_{set,clean}$ will be adopted to increase the loads P_{hvac}^t and P_{wh}^t. In this way, the clean energy can be consumed locally instead of being exported to the grid without any carbon offsetting benefit.

The predictive controllers (Figures 3 and 4) with and without carbon net-metering are similar to the corresponding momentary controllers in the initial steps. However, the predictive controllers utilize the emission data from the next timestep to further facilitate the control decisions. Essentially, when the emission level of the current timestep falls into the default range, the carbon emission of the next timestep CO_2^{t+1} is then compared with the LT and HT. If the next timestep is categorized as clean, the loads for the current timestep will be decreased to save for later, and vice versa. This algorithm enables more frequent setpoint adjustments and therefore leads to more shifting of loads to cleaner hours.

2.3. Co-simulation platform

A co-simulation platform is used for testing and validating the performance of the proposed control algorithms. The co-simulation platform is built on hierarchical engine for large-scale co-simulation (HELICS) tool [22]. Key capabilities such as high scalability, cross-platform operability, and modularity make HELICS suitable for developing co-simulation platforms. The co-simulation platform manages the data communication between different components of the closed-loop co-simulation. It is scalable and creates multiple agents depending on the number of houses in the simulated community.

Figure 5 depicts the components of the co-simulation platform and the data exchange flow between different components. Two types of agents are developed in this platform: (1) a building energy simulator (i.e., house agent) and (2) a carbon responsive controller agent. At the beginning of the simulation, an agent for the building simulation and an agent for the controller are instantiated simultaneously for each house.

Inside each house agent, we used the Operational, Controllable, High-resolution Residential Energy (OCHRE) model [23] for modeling the buildings in this study. OCHRE is capable of implementing the control signals for HVAC, WH, PV, and battery, and it is designed to be easily integrated into the co-simulation platform. More details about the community modeling are discussed in Section 3.

The data exchange between the house agent and the controller agent happens in the following order. At the beginning of timestep t, OCHRE computes the net house load (P_{net}^t), and the house agent sends P_{net}^t to the controller. At the same time, the controller agent receives the P_{net}^t together with the current carbon emission data from the Cambium database [24]. For predictive controllers, the future carbon emission data are also

received for computing the control actions with the assumption of perfect forecasts. The controller then computes the control setpoints based on the predetermined rules and sends it back to the house agent. After receiving the control action for each device from the controller agent, OCHRE implements the control action and proceeds to the next timestep $t + 1$.

3. Case study settings

3.1. Overview of the community

The Basalt Vista community, located in Basalt, Colorado, is modeled for the case study. This community is intended to provide affordable housing to schoolteachers in town while also being highly efficient all-electric homes with enough PV to make the community approximately net zero, as well as batteries for load shifting and resilience. Located at an elevation of 2,015 meters, it is in climate zone 7B, which is very cold and dry [25]. The community consists of 12 multifamily buildings, either duplexes or triplexes, with a total 27 homes. The homes consist of 2-, 3-, and 4-bedroom units, ranging from 107 to 156 square meters [26].

The HVAC systems of all the units are minisplit heat pump (MSHP) systems. The domestic hot water systems use heat pump water heaters (HPWH). Each unit is installed with rooftop PV systems, except for three units that do not have enough roof space for PV panels. The PV system sizes range from 7.6 to 11.85 kW. Among all the households, six homes are assumed to own electric vehicles and are equipped with Level 1 or Level 2 chargers. Four homes are equipped with home battery systems with capacities of 12 kWh.

3.2. Community modeling

The community is modeled in OCHRE [23], a control-oriented residential building modeling tool. Each building type (i.e., 2-, 3-, and 4-bedroom) share the same model formation with variant configuration parameters. The building envelope and the controllable loads (i.e., MSHP and HPWH) are described in this section. Models of PV, batteries, electric vehicles, and other electric loads can be found in reference [23].

The resistance-capacitance (RC) model is adopted for modeling the building envelope. R represents the thermal resistance between thermal masses, which involves both conduction and convection effects. C represents the thermal mass of different building components such as the air inside a room, exterior and interior walls, furniture, etc. The equation of a node i in the RC network is:

$$C_i \frac{dT_i^t}{dt} = \sum_{j=1}^{M} \frac{T_j^t - T_i^t}{R_{ij}} + H_i^t, \tag{1}$$

where C_i is the thermal mass of the node i, T_i^t is the temperature of node i, T_j^t is the temperature of node j adjacent to node i, R_{ij} is the thermal resistance between nodes i and j, H_i^t is the sensible heat injected to node i, and M is the total number of nodes in a house. For each house, approximately 13 Rs and 4 Cs were used to simulate the thermal dynamics. The detailed structure of the RC network model can be found in reference [23].

The MSHP in this work has a variable frequency drive that can modulate to maintain the setpoint of the conditioned space. A local proportional integral derivative controller adjusts the variable frequency drive's speed ratio according to the measured room temperature and the setpoint. For this community, the MSHPs are sized to be larger than might typically be sized according to standard sizing guidance such as the ACCA Manual J [27]. This is to ensure that the heat pump can fully meet the load even during the coldest hours of the year. With the oversized heat pumps, backup heaters are not installed, which makes these homes more energy efficient at the expense of a higher capital cost.

Further, each home has a highly efficient HPWH with backup electric resistance element installed. The heat pump itself is able to heat the tank more efficiently by removing heat from the ambient air and adding it to the tank. In contrast, the backup electric element is less efficient, but can heat the tank more quickly. When there is a demand for water heating, the heat pump turns on first. If there is a sufficiently large draw of hot water that the heat pump is unable to keep up, the backup electric element will then turn on. This will partially recover the tank temperature before switching back to the heat pump mode to maintain a high level of energy efficiency. The exact control sequence was derived from the detailed laboratory testing of this HPWH unit in response to different typical residential hot water draw profiles [28].

3.3. Inputs

The carbon emission data in this work are adopted from the Cambium data set [24]. Based on modeled futures of the U.S. electricity sector, Cambium assembles structured data sets of energy-related metrics (e.g., carbon emissions) to facilitate long-term decision-making. Specifically, the hourly short-run marginal carbon emission data from the Standard Scenarios 2020 Mid-case were adopted in the control development of this work. Though Cambium provides various scenario settings such as high vs. low renewable energy cost, we note that the simulated data are based on certain assumptions about the future projected U.S. electric sector. These assumptions are subject to many uncertainties, such as climate change and policy impacts, which could affect the results and analysis of this work.

Figure 6 visualizes the emissions data for the four selected simulation years from Cambium. We selected these four years because only even years are available in Cambium and we needed to avoid leap years as they are not yet supported in OCHRE. From the figure, we notice that as time goes by, more hours with zero or low carbon emissions emerge. This aligns with the increasing adoption rate of renewable energy and decarbonization measures of the electric sector. Regardless, we still observe some hours of high emission rate in year 2046, which represent the operation of coal-fired power plants. Because the emission data for the four years are different, we conducted a sensitivity analysis to determine the control thresholds (Section 4.2). As a result, we adopted the absolute values of the 30% and 70% of the emission range in 2022 as the LT and HT for all scenarios.

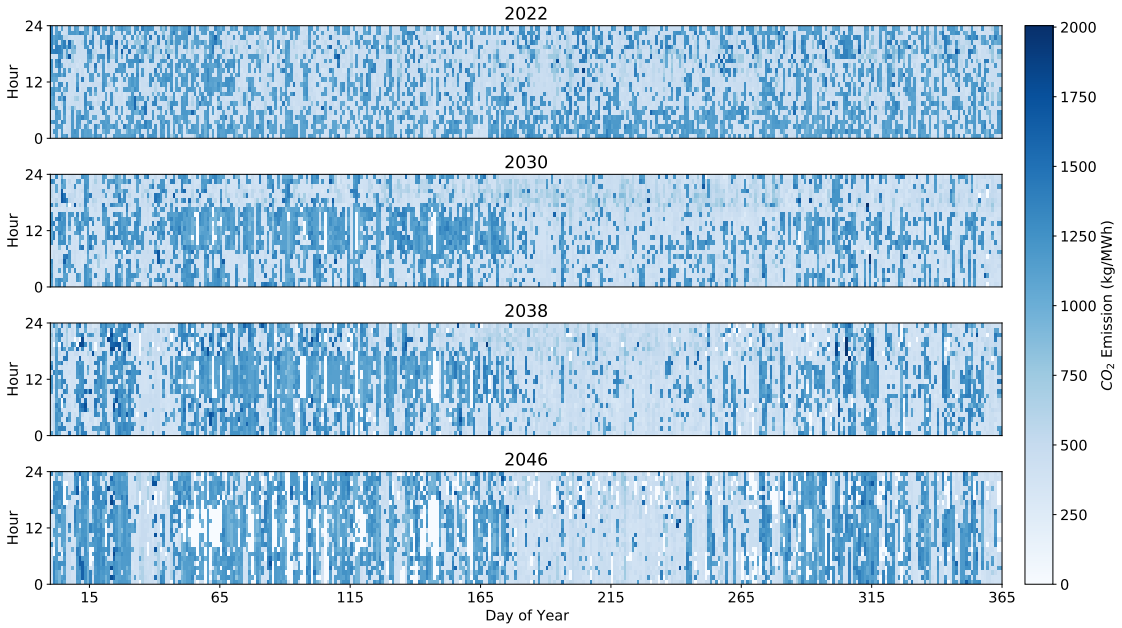

Figure 6: Emission data comparison across simulated years.

Similarly, the same weather data were used across all four simulation years to eliminate the impact of weather on building loads so that the results can be directly compared. Actual Meteorological Year (AMY) data of year 2012 for Pitkin County, Colorado, where the community is located, was used to be consistent with the Cambium weather data file. Here we note that forecasting future weather is an active research topic and is beyond the scope of this work. The occupancy, lighting, and appliance usage schedules for each house were generated from ResStock™ [29]. The time-of-use rate for the local electric utility Holy Cross Energy [30] was used for the energy cost calculation, where the on-peak (4–9 PM) price is \$0.24/kWh and the off-peak (rest of the hours) price is \$0.06/kWh.

3.4. Scenarios and evaluation metrics

Based on the case study settings proposed above, we designed five simulation scenarios to evaluate the controller performances. As seen in Table 3, the baseline scenario involves no carbon responsive building controller. The remaining four scenarios each adopts one carbon responsive controller proposed in Section 2, namely momentary or predictive rule-based controller with or without carbon net-metering. Annual energy simulations of the four selected years (2022, 2030, 2038, and 2046) were run with the default setpoints listed in Table 2. The house models were run with a timestep of 1 minute, and the control setpoints were updated with a 15-minute interval to avoid excessive cycling of the appliances.

To account for different carbon accounting methods, two ways to calculate the annual carbon emission are adopted. The first method is carbon net-metered, where the power exported to the grid can offset the total carbon emission. The second method does not take account of the exported power back to the grid. The equations for the two methods are as follows:

Table 3: Description of simulation scenarios in the case study.

Scenario	Carbon accounting method	Rule type	Year
Baseline	N/A	N/A	2022–2046
MO-0	Non-net-metering	Momentary	2022–2046
MO-1	Net-metering		
PR-0	Non-net-metering	Predictive	2022–2046
PR-1	Net-metering		

$$E_{net} = \sum_{t=1}^{N} e^t P^t_{net} \Delta t, \tag{2}$$

$$E_{non-net} = \sum_{t=1}^{N} e^t P^t_{net} \Delta t, \quad \forall\ P^t_{net} > 0, \tag{3}$$

where E_{net} and $E_{non-net}$ are the annual emission with and without carbon net-metering. t is the timestep, and N is the total number of timesteps in a year. e^t represents the real-time carbon emissions of the grid power. P^t_{net} is the net load of the house (i.e., total load subtracted by PV and battery power). Δt is the interval length of each timestep.

Thermal discomfort is quantified by the discomfort degree hours for the HVAC system. For HVAC heating scenarios, when the room temperature is below the heating setpoint, it is considered an uncomfortable time period, and vice versa. The switching between heating and cooling is dependent on the outdoor temperature. Note that in this paper we consider a setpoint not met as uncomfortable as the actual room temperature deviates from the predetermined setpoint. We did not adopt the ASHRAE recommended comfort range (i.e., 20–28°C) [31]

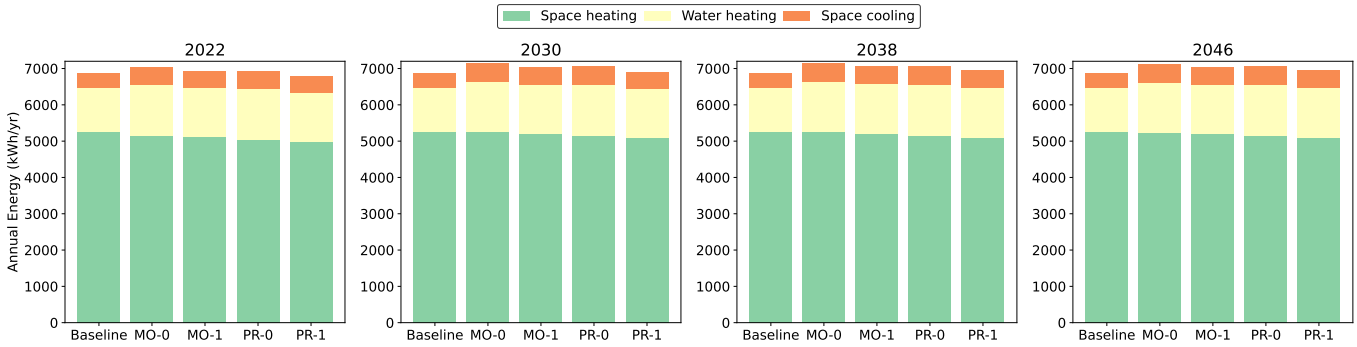

Figure 7: Community average annual energy consumption of controlled loads for different controllers across simulated years.

because it is relatively wide compared to our setpoints, which leads to almost the same level of discomfort in all scenarios. A list of the discomfort values according to the ASHRAE Standard is provided in Table A.2 in the appendix. The discomfort degree hours in this work can be defined by the following equation:

$$U_{hvac} = \sum_{t=1}^{N} |T^t_{indoor} - T^t_{set}|\,\Delta t, \quad \forall\ T^t_{indoor} < T^t_{set}\ (heating)\ and\ T^t_{indoor} > T^t_{set}\ (cooling), \tag{4}$$

where T_{indoor} and T_{set} are the actual indoor temperature and setpoint, and Δt is the simulation interval of the house model (i.e., 1 minute).

The thermal discomfort for WH is only considered for the shower in this work [32]. It is measured by the unmet thermal energy for any shower draws below 43.3°C (110°F), which is calculated by:

$$U_{wh} = \sum_{t=1}^{N} m^t_{water}\, c_p\, |T^t_{water} - 43.3|\,\Delta t, \quad \forall\ T^t_{water} < 43.3, \tag{5}$$

where m^t_{water} represents the hot water mass flow rate and T^t_{water} is the hot water temperature.

4. Results and discussions

4.1. Results

This subsection presents the annual simulation results with four performance metrics: energy consumption, carbon emission, energy cost, and thermal discomfort. Through the comparison of the four proposed controllers, we discuss the impact of carbon net-metering, as well as the effect of prediction in rule-based control. Additionally, we also investigate the evolution of results over the years.

4.1.1. Energy consumption

Figure 7 visualizes the community average annual energy consumption of the controlled loads (HVAC and WH) for different controllers. Compared to the baseline, the annual space heating energy consumption slightly decreases while both the space cooling and water heating energy increases. The divergent heating and cooling energy changes can be attributed to the higher emission levels in the heating season than those in the cooling season (see Figure 6), which leads to lower heating energy consumption. In general, carbon responsive building control increases the total household annual energy consumption.

Table 4: Community average annual energy consumption per household for different controllers across simulated years (percentage values are changes relative to the corresponding baseline).

Year	Baseline (kWh/yr)	MO-0	MO-1	PR-0	PR-1
2022	4,124	3.8%	1.3%	1.1%	-2.2%
2030	4,120	6.6%	3.7%	4.5%	0.9%
2038	4,108	6.7%	4.2%	4.7%	1.6%
2046	4,103	5.8%	3.7%	4.2%	1.6%

Table 4 lists the community average annual energy per household. In the table, the baseline energy consumption is shown in absolute values, whereas the other scenarios are in relative changes compared to the baseline. From the table, the average annual energy increase for the studied community is within 6.7%. For controllers accounting for carbon net-metering, the energy increase is about 2.5% to 3.0% lower compared to scenarios without carbon net-metering. This indicates the incentivizing impact of adopting carbon net-metering, as it encourages the exporting of power back to the grid. For controllers without carbon net-metering, the energy usage is increased when PV generation is excessive to increase the self-consumption rate, which has led to a higher annual energy consumption.

Another observation from Table 4 is that all predictive controllers perform better than the momentary controllers in terms of energy consumption. This is because the predictive controllers adjust the setpoints based on both current and future emission values. When the current carbon emission falls in the default zone but the future emission falls in the clean zone, it will reduce the current power, and vice versa. Because there are

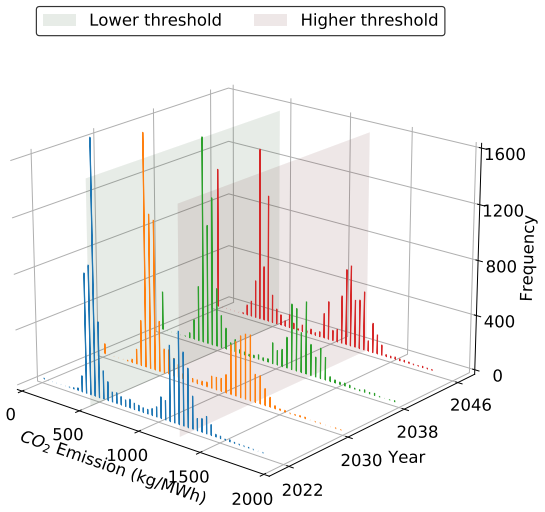

Figure 8: Histogram of carbon emission data for the simulated years.

more time instances classified as clean than carbon-intensive over the whole year (as shown in Figure 8), the predictive controllers therefore reduce energy consumption more often than increase it and save more energy compared to the momentary controllers.

4.1.2. Carbon emissions

Figure 9 illustrates the community average annual carbon emission of the controlled loads (HVAC and WH). From the figure, it can be seen that in all scenarios, the emissions caused by space heating are reduced through the carbon responsive control. In some scenarios, the emissions produced by cooling and water heating increased due to the corresponding energy increase. This is attributed to the fact that when there are consecutive clean hours, the controllers might pre-cool or pre-heat the space/water tank more than necessary, which leads to an increase of the total operational emissions. Overall, the annual household carbon emissions decreased compared to the baseline.

Table 5 lists the community average emission per household for different scenarios. In order to eliminate the impact of different carbon accounting methods and focus on the performance variance of the controllers, the carbon emission values listed in Table 5 are all net-metered (Equation 2). The emissions results calculated without carbon net-metering are presented in Table A.1 of the Appendix.

Based on Table 5, we can see that the controllers that consider carbon net-metering perform better than those that did not. This can be attributed to the logic of the controllers, where the non-net-metered controller increases the loads to do more pre-cooling/pre-heating when the house net-load is negative. This has led to a rise in energy as discussed in former sections, which hinders them from decreasing more carbon emissions.

Similar to the annual energy performance, the emission performance of the predictive controllers is better than the momentary ones. The reason is that predictive controllers make decisions informed by the emissions at the next timestep. This

Table 5: Community average annual carbon emission per household for different controllers across simulated years (net-metered; percentage values are changes relative to the corresponding baseline).

Year	Baseline (kg/yr)	MO-0	MO-1	PR-0	PR-1
2022	3,854	-6.0%	-11.0%	-6.8%	-12.1%
2030	2,158	-6.3%	-18.7%	-7.8%	-20.5%
2038	2,650	-6.5%	-15.2%	-7.7%	-16.5%
2046	3,453	-6.3%	-11.6%	-7.1%	-12.6%

enables a better shifting effect of loads to cleaner time periods than the momentary controllers. Cumulatively over a year, more emission is thus reduced by predictive controllers.

Overall, 6% to 20.5% annual carbon emissions reduction is seen by the proposed rule-based controllers compared to the baseline. In terms of the yearly change of emissions, it is interesting that year 2046 is not the one with the lowest emissions. According to Figure 8, though year 2046 has the most hours of zero emission, depending on the power profile of the houses, the zero emission hours might not align with the high-load hours. Figure 10 plots the heat map of a typical house's net load in year 2046. We see that the high-load hours are mostly in winter and during the nighttime, which align with the carbon-intensive hours in Figure 6. Therefore, it is safe to infer that the more the high-load hours align with the low-carbon hours, the lower the annual emissions will be.

4.1.3. Energy cost

Figure 11 plots the community average annual energy on- and off-peak costs of the controlled loads in 2022. Similar plots for the other simulation years can be found in Appendix A. From Figure 11, we can see that the on-peak energy costs all decreased and the off-peak costs all increased compared to the baseline. Figure 12 plots the house net load in response to the real-time emission signal on a sample winter day of a sample house. The figure shows that when the carbon emission of the on-peak hours exceeds the higher threshold at around 6 PM, the house net load drops below the baseline as all controllers lower the heating and WH setpoints to reduce the loads. However, a certain level of the rebound effect is seen later, where the controllers consume slightly more energy than the baseline due to the lower setpoints earlier. Overall, during the on-peak hours, more energy is saved due to the high emissions level. Over the whole year of simulation time, the on-peak hours are relatively more carbon-intensive and off-peak hours cleaner, which has led to the reduction of on-peak cost and increase of off-peak cost in Figure 11.

Table 6 summarizes the community average annual energy cost per household for each simulation year. Based on the table, all controllers that do not consider carbon net-metering perform better in terms of total cost. This can be attributed to the fact that controllers without net-metering tend to use more energy around noon (e.g., 11 AM to 3 PM in Figure 12) when the house net load is negative. Because of the rebound effect, they

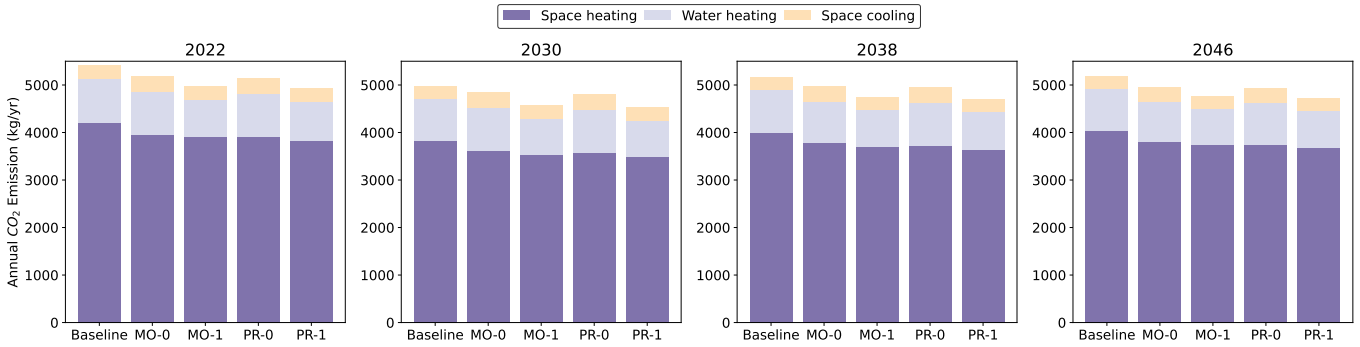

Figure 9: Community average annual carbon emission of controlled loads for different controllers across simulated years.

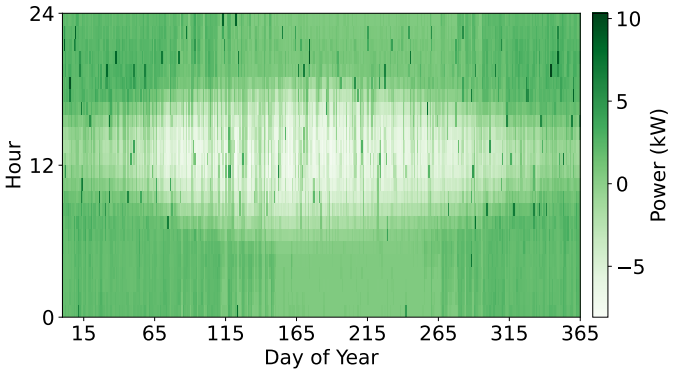

Figure 10: Annual house net load heat map (year 2046, house b5).

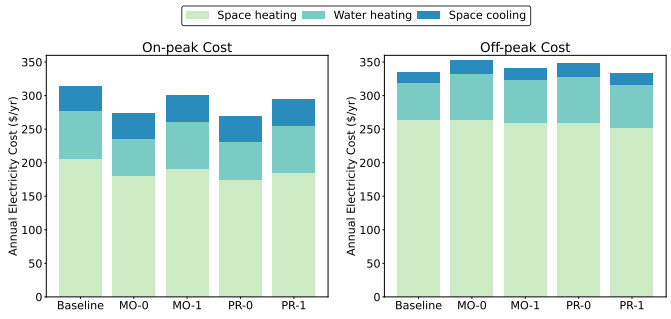

Figure 11: Community average annual energy on- and off-peak costs of controlled loads for different controllers in 2022.

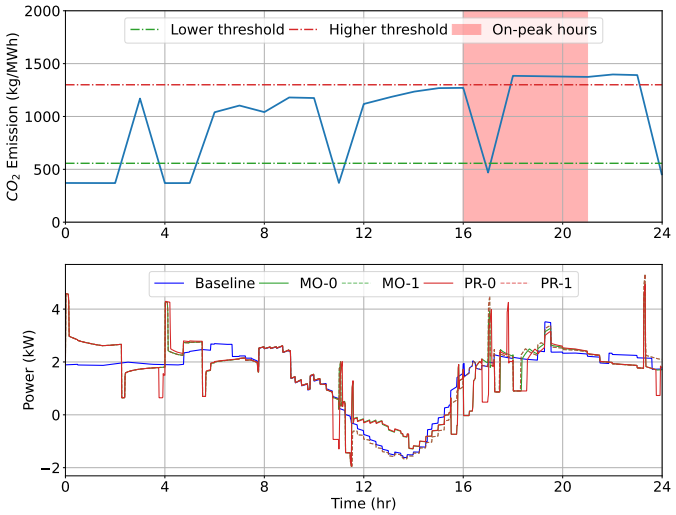

Figure 12: House net load in response to the emission signal (winter 2022, house b5).

Table 6: Community average annual energy cost per household for different controllers across simulated years (percentage values are changes relative to the corresponding baseline).

Year	Baseline ($/yr)	MO-0	MO-1	PR-0	PR-1
2022	718	-2.7%	-1.1%	-4.1%	-2.9%
2030	719	1.3%	3.4%	0.1%	1.7%
2038	717	0.5%	2.9%	-0.6%	1.3%
2046	715	-1.0%	1.2%	-1.8%	0.0%

will consume less energy later when PV generation decreases and the net load is positive. This enables shifting the load from on-peak hours to off-peak hours, which leads to more energy cost savings by the non-net-metered controllers. Additionally, all predictive controllers have more cost savings than the momentary ones. The reason is similar to the energy savings discussion in Section 4.1.1.

Generally, we see an annual energy cost change of -4.1% to 3.4% on top of the baseline. In terms of the yearly trend of cost savings, we notice that the cleaner the year, the less cost reduction potential. Here, clean means more hours of carbon emission under the lower threshold in Figure 8. More specifically, years 2030 and 2038 have more hours under the lower threshold, and the energy cost increased in all scenarios except one.

4.1.4. Thermal discomfort

Table 7 lists the heating, cooling, and water heating discomfort values for all scenarios across the simulation years. From the table, we see that carbon responsive control brings in a higher level of discomfort in space heating and cooling compared to the baseline, where constant setpoints were implemented annually. However, the hot water discomfort has been

Table 7: Community average heating, cooling, and water heating discomfort metric values for each simulation scenario.

Year	Heating (°C-hrs/yr)					Cooling (°C-hrs/yr)					Hot water (kWh/yr)				
	Baseline	MO-0	MO-1	PR-0	PR-1	Baseline	MO-0	MO-1	PR-0	PR-1	Baseline	MO-0	MO-1	PR-0	PR-1
2022	8	24	27	30	33	0	2.2	4.1	1.9	3.4	1.3	0.15	0.23	0.19	0.25
2030	8	34	40	31	36	0	1.0	4.4	1.0	3.5	1.3	0.26	0.40	0.26	0.37
2038	8	69	79	64	73	0	1.7	7.5	1.5	6.0	1.3	0.37	0.57	0.39	0.58
2046	8	55	66	51	59	0	2.8	6.8	2.4	5.6	1.3	0.37	0.64	0.31	0.56

slightly improved, which is validated through a higher annual average hot water temperature. Generally, the annual discomfort levels in all the carbon responsive scenarios are maintained within an acceptable range.

When carbon net-metering is considered in the control, the discomfort level increases compared to scenarios without net-metering. This is because when power exporting does not bring emission benefits, the controller tries to increase the self-consumption rate of the surplus PV generation by consuming more energy. This has led to a relatively higher indoor temperature in the heating season and a relatively lower temperature in the cooling season, which means a more comfortable indoor environment for the occupants.

Comparing scenarios with and without predictive control, we notice that predictive control can lead to either an increase or decrease of the discomfort level. There is no direct correlation between the two. Though predictive controllers look ahead for one timestep, the decision to increase or decrease the setpoints is dependent on the emission level at the next timestep, which is rather stochastic in the time frame of one year of simulation time.

4.2. Sensitivity analysis

Control thresholds. The choice of the lower and upper thresholds in rule-based control is essential. To investigate how the thresholds affect the control performance, we conducted a sensitivity analysis. The original lower and upper thresholds were adjusted based on the simulation scenario MO-1 2022. A list of the control performance metrics can be found in Table 8. The percentages (e.g., 10&90) here represent the LT and HT, which are based on the emission data range of 2022. The same absolute values of the LT and HT were used across different years.

From the table, carbon emissions decrease while the control threshold range gets narrower. Specifically, the emission drops drastically from thresholds 20&80 to 30&70 because the latter is more sensitive to emission changes, which leads to more frequent carbon responsive setpoint adjustments.

The relationship between energy consumption and the thresholds is less explicit. Given the same emission signal input, the closer the thresholds, the more hours that fall out of the default zone. Hence, the energy consumption variation depends on the distribution of the emission data. For instance, when the thresholds change from 20&80 to 30&70, more hours are becoming clean compared to hours that are becoming carbon-intensive. This leads to more energy consumed over the whole year.

Table 8: Comparison of average performance metric values per household with various control thresholds.

		Lower & upper threshold percentages			
		10&90	20&80	30&70	40&60
Emission (kg/yr)		3,852	3,819	3,429	3,088
Energy (kWh/yr)		4,123	4,106	4,177	4,046
Total energy cost ($/yr)		718	715	711	706
On-peak cost ($/yr)		627	625	613	617
Off-peak cost ($/yr)		91	90	97	88
Discomfort	Heating (°C-hrs/yr)	8	11	27	238
	Cooling (°C-hrs/yr)	0	0.1	4	21
	Hot water (kWh/yr)	1.3	1.2	0.2	0.9

The annual energy cost sinks with the narrowing threshold range, making the 40&60 thresholds the most cost-effective range. However, the zone thermal discomfort level also reaches the highest in the 40&60 range. This is because the frequent thermostat changes cause the room temperature to swing so that it is more likely to fall outside the comfort zone. The hot water temperature depends not only on the setpoint but also the water draw profile. There is therefore no explicit correlation between the hot water discomfort level and the thresholds.

To summarize, the 30&70 lower and upper control thresholds chosen in this work best balance the benefits of emissions reduction and energy cost, as well as thermal comfort for the homeowners.

Control interval. The impact of control interval is studied through varied intervals based on scenario MO-1 2022. From Table 9, we observe that the performance of the 15-minute and 30-minute control intervals is very similar to each other. The 15-minute interval performs better at energy and comfort, whereas the 30-minute is better at emissions and cost. When the interval becomes larger than 30 minutes (e.g., 60 minutes and 120 minutes), then the larger the interval, the worse the control performance. This is probably because in these cases, the controller changes the setpoints too infrequently, which hinders the benefits of carbon responsive control. Considering the

Table 9: Comparison of average performance metric values per household with various control intervals.

		Control interval (minute)			
		15	30	60	120
Emission (kg/yr)		3,429	3,387	3,480	3,740
Energy (kWh/yr)		4,177	4,184	4,240	4,329
Total energy cost ($/yr)		711	710	714	724
On-peak cost ($/yr)		613	612	613	619
Off-peak cost ($/yr)		97	98	101	105
Discomfort	Heating (°C-hrs/yr)	27	31	38	49
	Cooling (°C-hrs/yr)	4	5	6	12
	Hot water (kWh/yr)	0.2	0.2	0.2	0.3

balance between control performance and the building thermal dynamics, we chose the control interval to be 15 minutes.

5. Conclusion

In this paper, we propose a carbon emission responsive control framework for thermostatically controlled loads. Within this framework, the four various controllers adjust thermostat setpoints according to projected carbon emission signals. The impact of carbon net-metering in both momentary and predictive rule-based controllers is investigated through the controller design and a case study. Sensitivity analysis is conducted to evaluate the role of control thresholds and control interval in the controller design.

Based on the simulation results, the average annual household carbon emissions are decreased by 6.0% to 20.5% compared to the baseline. The average annual energy consumption is increased by less than 6.7% due to more clean hours over the year. The annual energy cost change lies between -4.1% and 3.4% on top of the baseline. All on-peak energy costs decreased while all off-peak costs increased, indicating that the carbon intensities during on-peak hours are higher than those during off-peak hours. Generally, the annual discomfort levels in all the carbon responsive scenarios are maintained within an acceptable range.

Evaluating the impact of carbon net-metering, we found that controllers with carbon net-metering show 2.5% to 3.0% less energy consumption and 5% to 12.7% less emission than controllers without carbon net-metering. This indicates the incentivizing impact of adopting carbon net-metering, as it encourages the exporting of power back to the grid. For controllers without carbon net-metering, higher annual energy consumption and carbon emissions result from attempting to increase the PV self-consumption rate. However, all controllers that do not consider carbon net-metering perform better in terms of the total cost. Due to the rebound effect, they tend to be shifting loads from on-peak hours to off-peak hours, causing the total cost to sink. Further, because more energy is consumed, non-net-metering controllers tend to create a more comfortable indoor environment for the occupants.

All predictive controllers perform better than the momentary controllers in terms of energy consumption, carbon emission, and energy cost. This is attributed to the enhanced load shifting effect by the predictive controller design. Also, this finding verifies the claim in reference [21] that predictive rule-based controllers are promising alternatives to optimization-based controllers because they are simpler and still effective.

We notice in some scenarios the emissions produced by space cooling and water heating are higher compared to the baseline due to the increased energy consumption from load shifting. This indicates rule-based control solely informed by carbon emission signals may end up with higher emissions, which could be overcome by using optimization-based control methods such as MPC.

Future work includes:

- Investigating better designs of the control rules to achieve synergetic emission, energy, and cost reductions.
- Incorporating other types of controllable loads such as schedulable loads into the carbon emission responsive control framework.
- Comparing the performance of the developed rule-based control to optimization-based control.

Acknowledgements

This work was authored by the National Renewable Energy Laboratory, operated by Alliance for Sustainable Energy, LLC, for the U.S. Department of Energy (DOE) under Contract No. DE-AC36-08GO28308. Funding provided by the U.S. Department of Energy Office of Energy Efficiency and Renewable Energy Building Technologies Office. The views expressed in the article do not necessarily represent the views of the DOE or the U.S. Government. The U.S. Government retains and the publisher, by accepting the article for publication, acknowledges that the U.S. Government retains a nonexclusive, paid-up, irrevocable, worldwide license to publish or reproduce the published form of this work, or allow others to do so, for U.S. Government purposes. This research was also partially supported by the National Science Foundation under Awards No. CBET-2217410. The authors would like to gratefully acknowledge Holy Cross Energy and Habitat for Humanity Roaring Fork Valley for providing the building floor plans and the site plan of the community, the AMI data, and collaborative discussions.

Appendix A.

Table A.1: Community average annual carbon emission per household for different controllers across simulated years (non-net-metered; percentage values are changes relative to the corresponding baseline).

Year	Baseline (kg/yr)	MO-0	MO-1	PR-0	PR-1
2022	8,318	-5.1%	-4.0%	-5.4%	-4.4%
2030	7,201	-4.6%	-3.4%	-4.9%	-3.8%
2038	7,476	-5.0%	-3.6%	-5.3%	-4.0%
2046	7,793	-5.4%	-4.0%	-5.8%	-4.3%

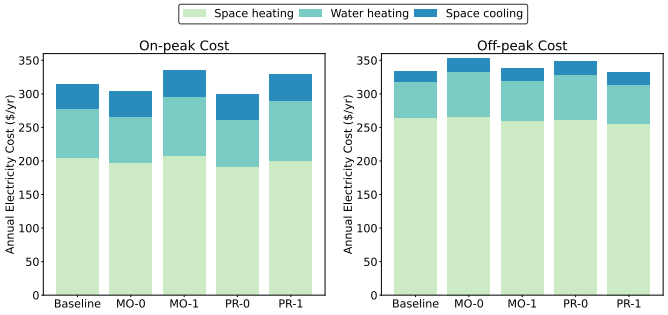

Figure A.1: Community average annual energy on- and off-peak costs of controlled loads for different controllers in 2030.

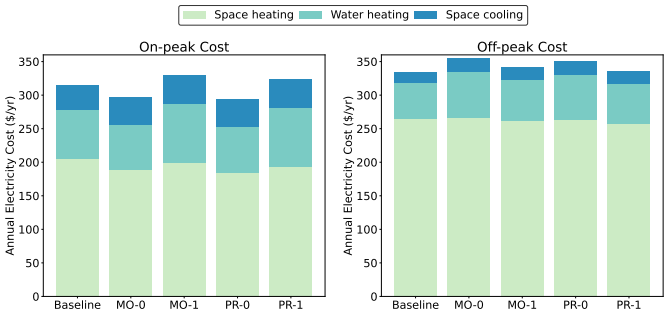

Figure A.2: Community average annual energy on- and off-peak costs of controlled loads for different controllers in 2038.

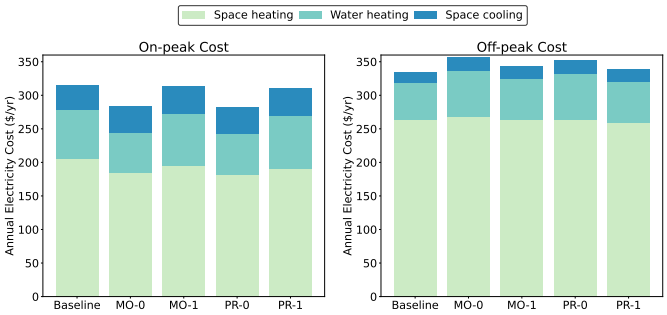

Figure A.3: Community average annual energy on- and off-peak costs of controlled loads for different controllers in 2046.

Table A.2: Community average indoor discomfort values for each simulation scenario based on ASHRAE Standard 55.

Year	ASHRAE discomfort (°C-hrs/yr)				
	Baseline	MO-0	MO-1	PR-0	PR-1
2022	3.8	3.5	3.5	3.9	3.9
2030	3.8	2.1	2.1	2.1	2.1
2038	3.8	3.2	3.3	3.3	3.3
2046	3.8	3.1	3.2	3.7	3.8

References

[1] U.S. Energy Information Administration, U.S. energy-related carbon dioxide emissions, 2019, Tech. rep. (2020).

[2] The White House, Fact sheet: President Biden sets 2030 greenhouse gas pollution reduction target aimed at creating good-paying union jobs and securing U.S. leadership on clean energy technologies, accessed 9 July 2021 (2021).
URL https://www.whitehouse.gov/briefing-room/statements-releases/2021/04/22/fact-sheet-president-biden-sets-2030-greenhouse-gas-pollution-reduction-target-aimed-at-creating-good-paying-union-jobs-and-securing-u-s-leadership-on-clean-energy-technologies/

[3] A. Satchwell, M. A. Piette, A. Khandekar, J. Granderson, N. M. Frick, R. Hledik, A. Faruqui, L. Lam, S. Ross, J. Cohen, K. Wang, D. Urigwe, D. Delurey, M. Neukomm, D. Nemtzow, A national roadmap for grid-interactive efficient buildings, Tech. rep. (2021). doi:https://doi.org/10.2172/1784302.

[4] G. Legorburu, A. D. Smith, Incorporating observed data into early design energy models for life cycle cost and carbon emissions analysis of campus buildings, Energy and Buildings 224 (2020) 110279. doi:https://doi.org/10.1016/j.enbuild.2020.110279.

[5] Y. Cang, Z. Luo, L. Yang, B. Han, A new method for calculating the embodied carbon emissions from buildings in schematic design: Taking "building element" as basic unit, Building and Environment 185 (2020) 107306. doi:https://doi.org/10.1016/j.buildenv.2020.107306.

[6] M. Almeida, M. Ferreira, Ten questions concerning cost-effective energy and carbon emissions optimization in building renovation, Building and Environment 143 (2018) 15–23. doi:https://doi.org/10.1016/j.buildenv.2018.06.036.

[7] S. M. Garriga, M. Dabbagh, M. Krarti, Optimal carbon-neutral retrofit of residential communities in Barcelona, Spain, Energy and Buildings 208 (2020) 109651. doi:https://doi.org/10.1016/j.enbuild.2019.109651.

[8] J. Langevin, C. B. Harris, J. L. Reyna, Assessing the potential to reduce US building CO_2 emissions 80% by 2050, Joule 3 (10) (2019) 2403–2424. doi:https://doi.org/10.1016/j.joule.2019.07.013.

[9] A. Fathy, A. Salib, M. Krarti, Transitioning from net-zero energy homes to carbon-neutral grid-connected communities, ASME Journal of Engineering for Sustainable Buildings and Cities 1 (4) (2020). doi:https://doi.org/10.1115/1.4049074.

[10] Y. Lou, Y. Yang, Y. Ye, W. Zuo, J. Wang, The effect of building retrofit measures on co_2 emission reduction–a case study with US medium office buildings, Energy and Buildings 253 (2021) 111514.

[11] T. Renugadevi, K. Geetha, K. Muthukumar, Z. W. Geem, Optimized energy cost and carbon emission-aware virtual machine allocation in sustainable data centers, Sustainability 12 (16) (2020) 6383. doi:https://doi.org/10.3390/su12166383.

[12] H. Ghazzai, A. Kadri, Joint demand-side management in smart grid for green collaborative mobile operators under dynamic pricing and fairness

setup, IEEE Transactions on Green Communications and Networking 1 (1) (2016) 74–88. doi:https://doi.org/10.1109/tgcn.2016.2646818.

[13] Z. T. Olivieri, K. McConky, Optimization of residential battery energy storage system scheduling for cost and emissions reductions, Energy and Buildings 210 (2020) 109787. doi:https://doi.org/10.1016/j.enbuild.2020.109787.

[14] T. Péan, R. Costa-Castelló, J. Salom, Price and carbon-based energy flexibility of residential heating and cooling loads using model predictive control, Sustainable Cities and Society 50 (2019) 101579. doi:https://doi.org/10.1016/j.scs.2019.101579.

[15] J. Gasser, H. Cai, S. Karagiannopoulos, P. Heer, G. Hug, Predictive energy management of residential buildings while self-reporting flexibility envelope, Applied Energy 288 (2021) 116653. doi:https://doi.org/10.1016/j.apenergy.2021.116653.

[16] X. Jin, K. Baker, D. Christensen, S. Isley, Foresee: A user-centric home energy management system for energy efficiency and demand response, Applied Energy 205 (2017) 1583–1595. doi:https://doi.org/10.1016/j.apenergy.2017.08.166.

[17] K. Leerbeck, P. Bacher, R. G. Junker, A. Tveit, O. Corradi, H. Madsen, R. Ebrahimy, Control of heat pumps with CO_2 emission intensity forecasts, Energies 13 (11) (2020) 2851. doi:https://doi.org/10.3390/en13112851.

[18] J. Clauß, S. Stinner, I. Sartori, L. Georges, Predictive rule-based control to activate the energy flexibility of Norwegian residential buildings: Case of an air-source heat pump and direct electric heating, Applied Energy 237 (2019) 500–518. doi:https://doi.org/10.1016/j.apenergy.2018.12.074.

[19] X. Zhang, Y. Wang, How to reduce household carbon emissions: A review of experience and policy design considerations, Energy Policy 102 (2017) 116–124. doi:https://doi.org/10.1016/j.enpol.2016.12.010.

[20] B. Alimohammadisagvand, J. Jokisalo, K. Sirén, Comparison of four rule-based demand response control algorithms in an electrically and heat pump-heated residential building, Applied Energy 209 (2018) 167–179. doi:https://doi.org/10.1016/j.apenergy.2017.10.088.

[21] D. Fischer, H. Madani, On heat pumps in smart grids: A review, Renewable and Sustainable Energy Reviews 70 (2017) 342–357. doi:https://doi.org/10.1016/j.rser.2016.11.182.

[22] B. Palmintier, D. Krishnamurthy, P. Top, S. Smith, J. Daily, J. Fuller, Design of the HELICS high-performance transmission-distribution-communication-market co-simulation framework, in: 2017 Workshop on Modeling and Simulation of Cyber-Physical Energy Systems (MSCPES), IEEE, 2017, pp. 1–6. doi:https://doi.org/10.1109/mscpes.2017.8064542.

[23] M. Blonsky, J. Maguire, K. McKenna, D. Cutler, S. P. Balamurugan, X. Jin, OCHRE: The object-oriented, controllable, high-resolution residential energy model for dynamic integration studies, Applied Energy 290 (2021) 116732. doi:https://doi.org/10.1016/j.apenergy.2021.116732.

[24] P. Gagnon, W. Frazier, E. Hale, W. Cole, Cambium documentation: Version 2020, Tech. rep., National Renewable Energy Laboratory (2020).

[25] The American Society of Heating, Refrigerating and Air-Conditioning Engineers, ASHRAE Standard 169-2006: Weather data for building design standards (2006).

[26] Aspen/Pitkin County Housing Authority, Basalt Vista housing, accessed 30 June 2021 (2021).
URL https://www.apcha.org/374/Basalt-Vista-Housing/

[27] Air Conditioning Contractors of America (ACCA), Manual J: Residential load calculation, Tech. report, ACCA (2008).

[28] B. Sparn, K. Hudon, D. Christensen, Laboratory performance evaluation of residential integrated heat pump water heaters, Tech. rep., National Renewable Energy Laboratory (2014).

[29] E. Wilson, C. Christensen, S. Horowitz, J. Robertson, J. Maguire, Energy efficiency potential in the U.S. single-family housing stock, Tech. rep., National Renewable Energy Laboratory (2017).

[30] Holy Cross Energy, Holy Cross Energy electric service tariffs, rules and regulations, accessed 8 July 2021 (2021).
URL https://www.holycross.com/wp-content/uploads/2018/12/Electric-Service-Tariffs-Rules-and-Regulations-12.17.2018.pdf

[31] The American Society of Heating, Refrigerating and Air-Conditioning Engineers, ASHRAEstandard 55 – thermal environmental conditions for human occupancy (2020).

[32] J. Maguire, How hot is hot enough? Quantifying unmet loads in simulation, in: 2020 ACEEE Hot Water Forum, ACEEE, 2020.